Electronic Supplementary Material (ESI) for Lab on a Chip.

Supplementary Information for

Bacterial classification and antibiotic susceptibility testing on an integrated microfluidic platform

Alexandros A. Sklavounos[a,b,†], Carine R. Nemr[a,†], Shana O. Kelley[a,c,d], Aaron R. Wheeler*[a,b,c]

a. Department of Chemistry, University of Toronto, 80 Saint George Street, Toronto, Ontario, M5S 3H6, Canada.
b. Donnelly Centre for Cellular and Biomolecular Research, University of Toronto, 160 College Street, Toronto, Ontario, M5S 3G9, Canada.
c. Institute of Biomedical Engineering, University of Toronto, 164 College Street, Toronto, Ontario, M5S 3G9, Canada.
d. Department of Pharmaceutical Science, University of Toronto, 144 College Street, Toronto, Ontario, M5S 3E5, Canada.

† A.A.S. and C.R.N. contributed equally.

* Corresponding author email address: aaron.wheeler@utoronto.ca

This PDF file includes:

AST via standard broth microdilution assay

Ciprofloxacin stock solutions were prepared in distilled water, while nitrofurantoin stock solutions were prepared in N,N-dimethylformamide. Broth microdilution assays were performed following standard protocols (Wiegand et al., *Nature Protocols*., 2008, **3**, 163–175). Briefly, ten 2-fold antibiotic dilution series, as well as solutions without antibiotics for growth controls (GCs) and sterility controls (SCs), were added to 96-well plates. Solutions were diluted 1:1 with either 10^6 CFU/mL bacterial suspensions in MHB or with MHB alone (SCs). After 16 – 20 h at 37 °C, OD_{600} measurements were obtained to determine the MIC of each antibiotic, which was defined as the minimum concentration tested that resulted in a percent viability ≤ 20% (Azizi et al., *Analytical Chemistry*., 2018, **90**, 14137–14144) according to the following equation.

$$\%\ viability = 100\% \times \frac{OD_{600,\,Sample} - OD_{600,SC}}{OD_{600,GC} - OD_{600,SC}}$$

Equation S1. Percent viability calculation from OD_{600} measurements, where $OD_{600,Sample}$ is the measurement of a sample with a specified antibiotic concentration, $OD_{600,SC}$ is the measurement of the SC and $OD_{600,GC}$ is the measurement of the GC.

Monitoring resazurin conversion to resorufin in plate reader

To evaluate the relationship between resorufin fluorescence mid-point time and bacterial inoculation density, 100 µL aliquots of *E. coli* CFT073 dilutions at different densities in 0.25 mM resazurin in MHB containing 0.1% wt/wt Tetronic 90R4 were added to wells in 96-well plates. Fluorescence ($\lambda_{ex}/\lambda_{em}$ = 565 nm/585 nm) was monitored over 19 h on a Cytation 5 multi-mode reader (BioTek).

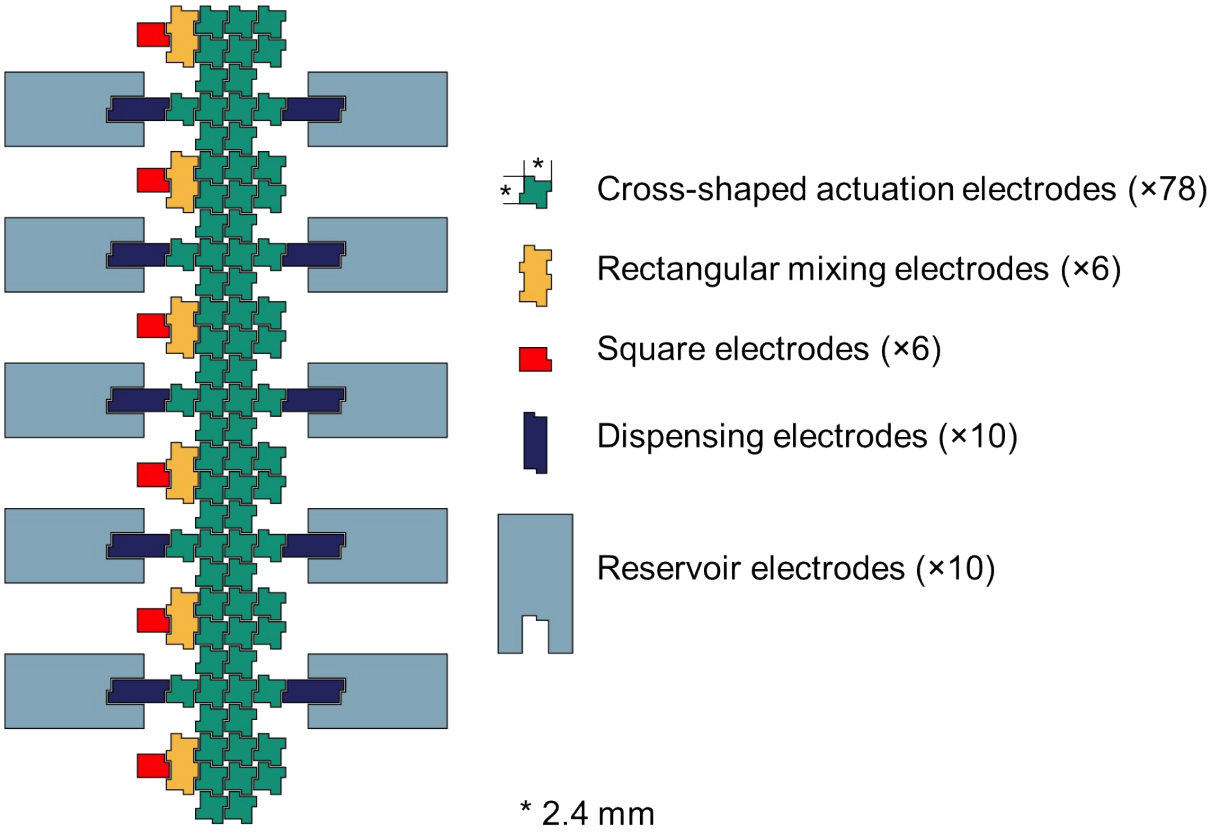

Fig. S1. Top-view cartoon of DMF device bottom plate design. The bottom plate features an array of 78 cross-shaped actuation electrodes (green), 6 rectangular mixing electrodes (yellow), 6 square electrodes (red), 10 rectangular dispensing electrodes (navy blue), and 10 reservoir electrodes (light blue).

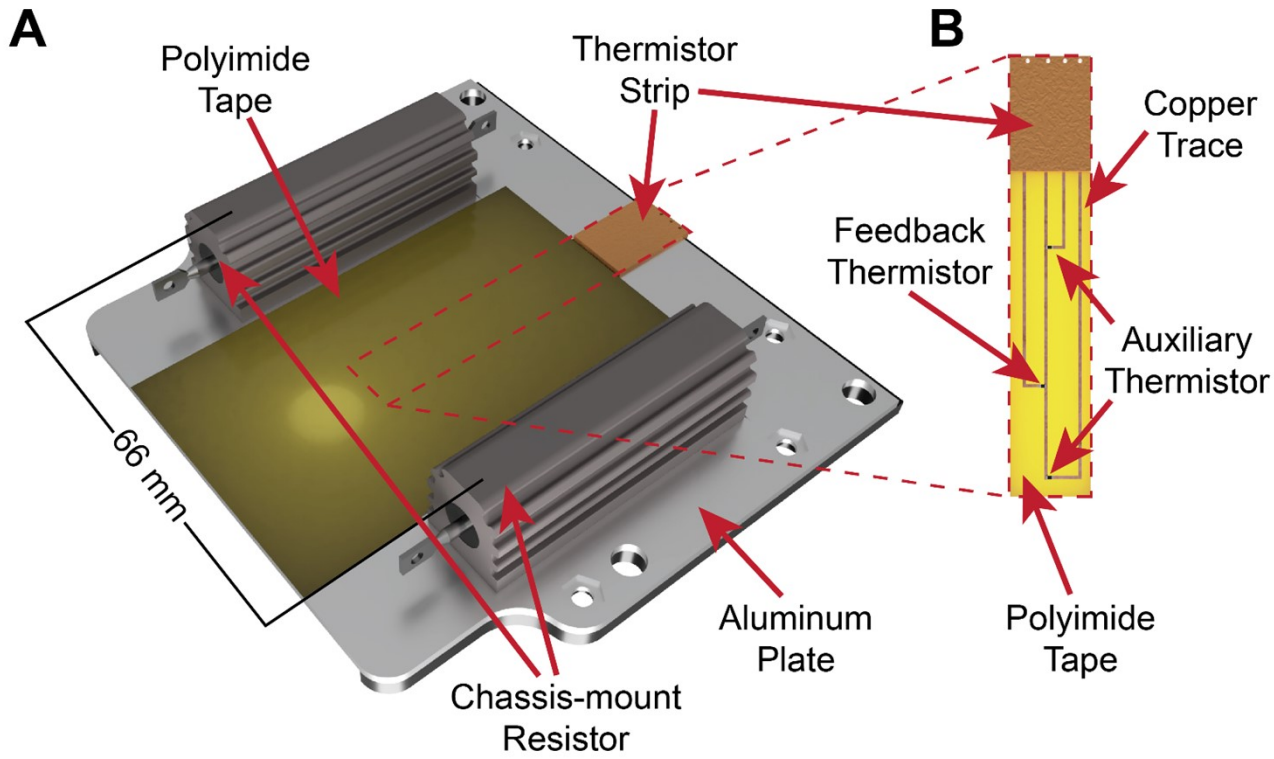

Fig. S2. Rendered image of the back side of the integrated heating unit in the DMF control system. (A) The heating unit comprised an aluminium plate (108 mm × 95 mm × 1.65 mm) on which two chassis-mount resistors were attached 66 mm apart. A thermistor strip was placed in between the plate and a layer of polyimide (Kapton®) film, to protect the thermistor from wear. (B) The thermistor strip comprised a polyimide (Kapton®) film coated with copper. The film was patterned in-house to serve as wiring for the thermistors. Three Negative Temperature Coefficient thermistors (one feedback and two auxiliary thermistors) were soldered on the copper wires.

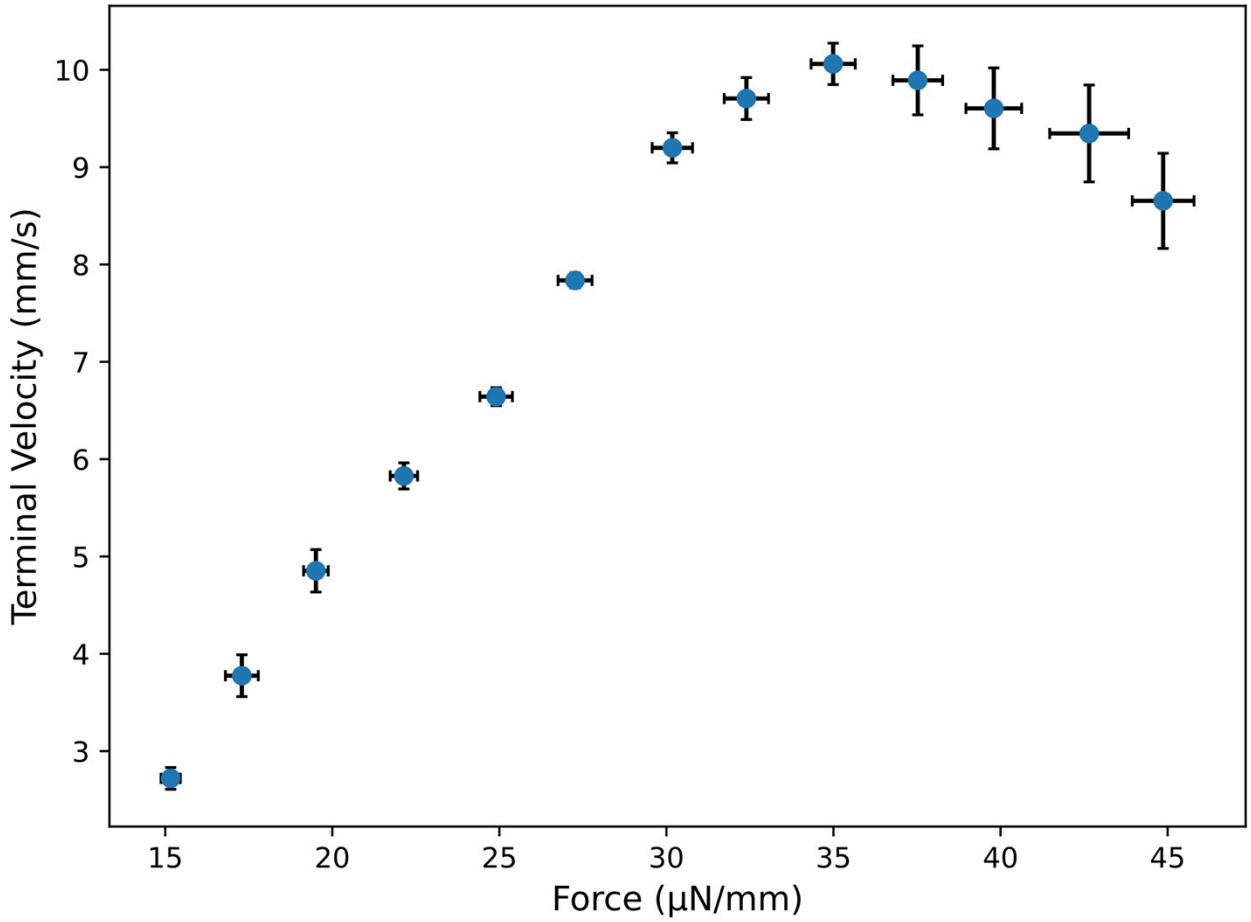

Fig. S3. Force-velocity plot of unit-volume droplets of assay diluent on the DMF devices used here, implemented as described in Swyer et al., *Langmuir*., 2019, **35**, 5342–5352. Error bars represent ± standard deviation of n = 10 measurements.

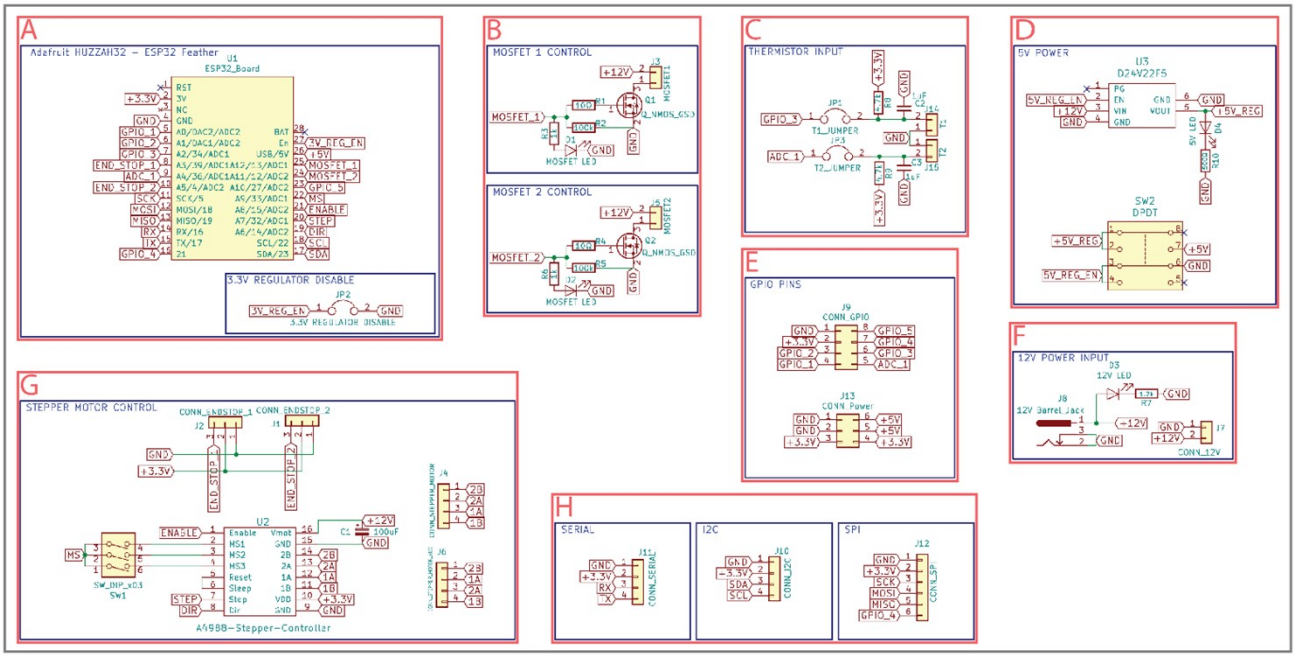

Fig. S4. Schematic and pinout drawings of the custom GPIO board used in the DMF control system. The board includes: (A) a socket for the microcontroller board HUZZAH32 – ESP32, (B) two high power transistors (MOSFETs), (C) a set of two thermistor inputs (not used in this study), (D) a 12 V to 5 V step down (for standalone operation of the board), (E) input and output pins of the microcontroller board exposed to male header pins for easy access, (F) a 12 V input jack, (G) a stepper driver socket (for controlling a stepper motor, not used in this study), and (H) sets of digital communication ports (SRIAL, I2C & SPI) bundled in male header pins for convenience. The microcontroller was used to modulate the two transistor units (to set the state and intensity of the white and green LED strips) and the filter slider (using the SERIAL communication protocol). The board is powered by a 12 V power supply and can exchange data with another device (*e.g.*, host computer) over USB, Bluetooth or Wi-Fi. In this study, Bluetooth communication was employed.

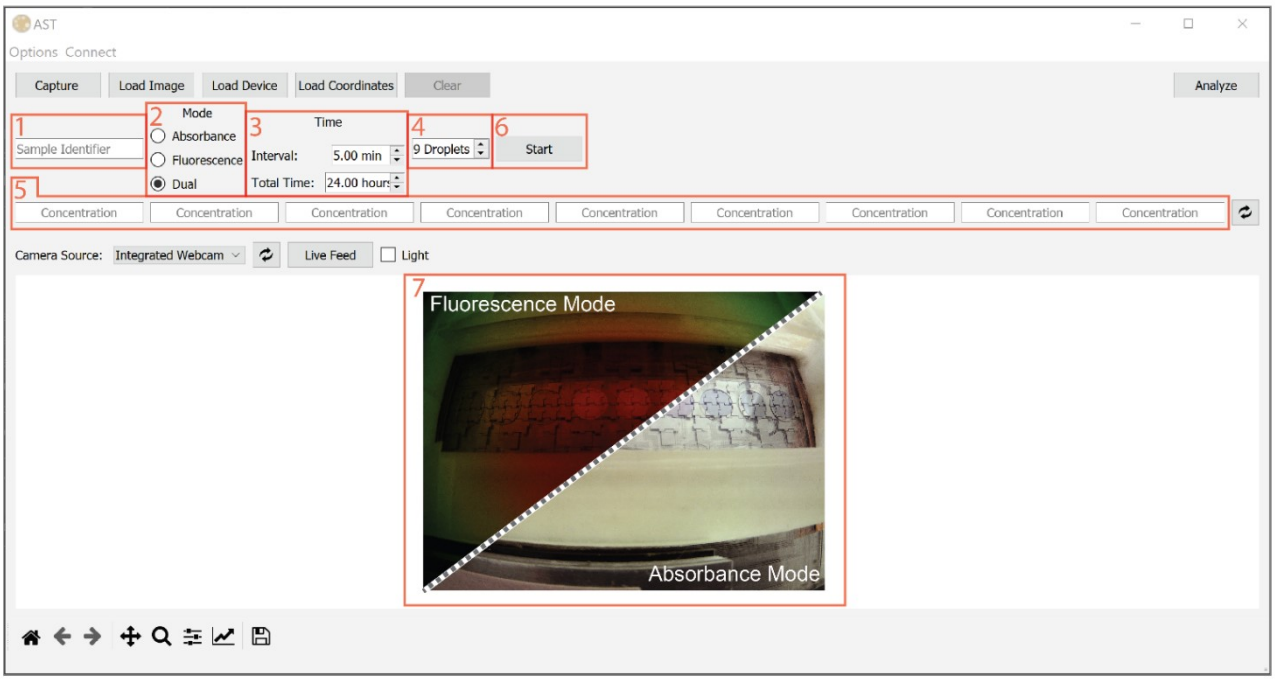

Fig. S5. Screenshot of custom user interface (UI), which provides space for the seven tasks. (1) The user can name the sample being tested. (2) The user has Bluetooth remote control of the GPIO board (LEDs and filter slider position), which includes bundled controls for fluorescence mode (turn on green LEDs, move slider to filter position and set camera exposure time to 640 ms), absorbance mode (turn on white LEDs, move slider to no filter position and set camera exposure time to 2.5 ms) and dual mode (absorbance mode followed by fluorescence mode). (3) The user can set the interval and total duration of image capture from the USB camera to desired times. (4) The user can specify the maximum number of sample-droplets on the DMF device; up to nine four-unit droplets (4.4 µL) can be incubated on the chip used in this study. (5) Droplets are annotated with desired labels (*e.g.*, antibiotic concentration, SC, GC, BCsubstrate). (6) The Start button allows the user to initiate the experiment timer. (7) The user sees a display of most recent captured image in fluorescence (as illustrated above the dashed white line) or absorbance mode (below the dashed white line).

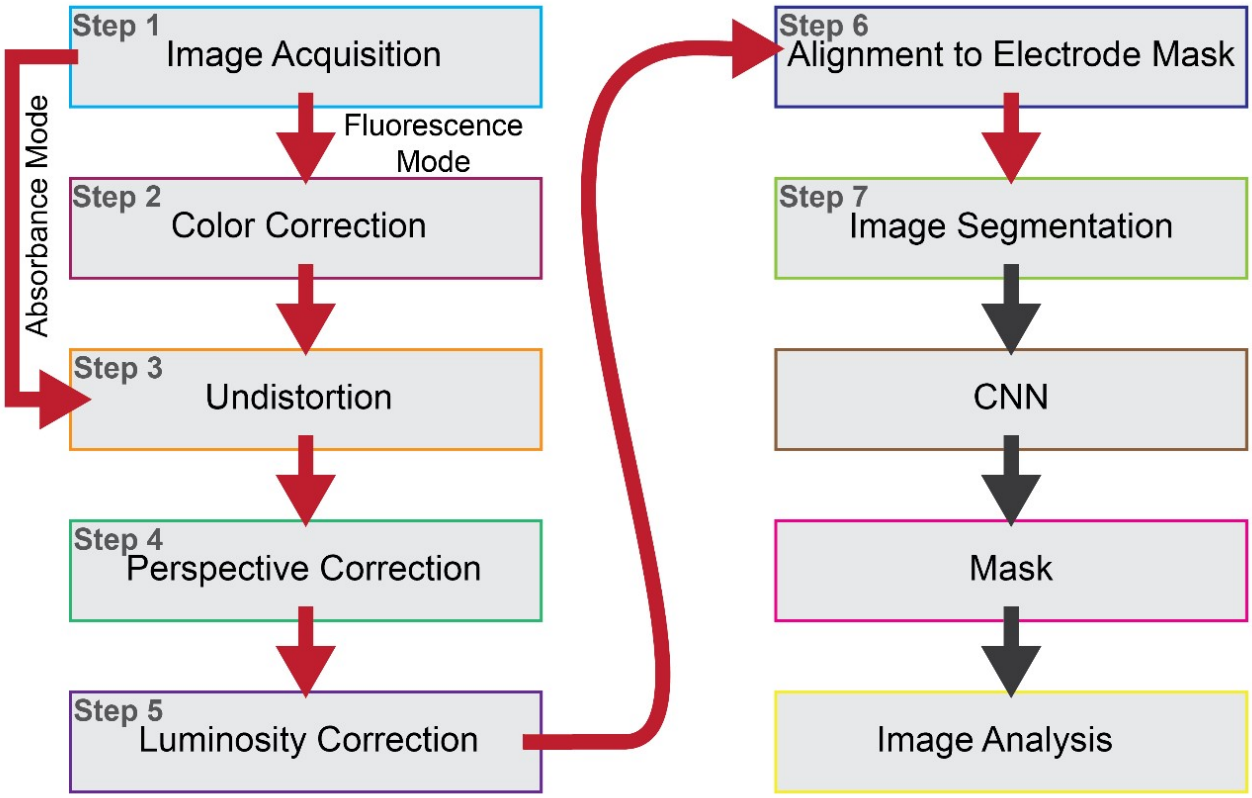

Fig. S6. Flowchart illustrating the custom image pre-processing (red arrows) and AI/processing steps (black arrows).

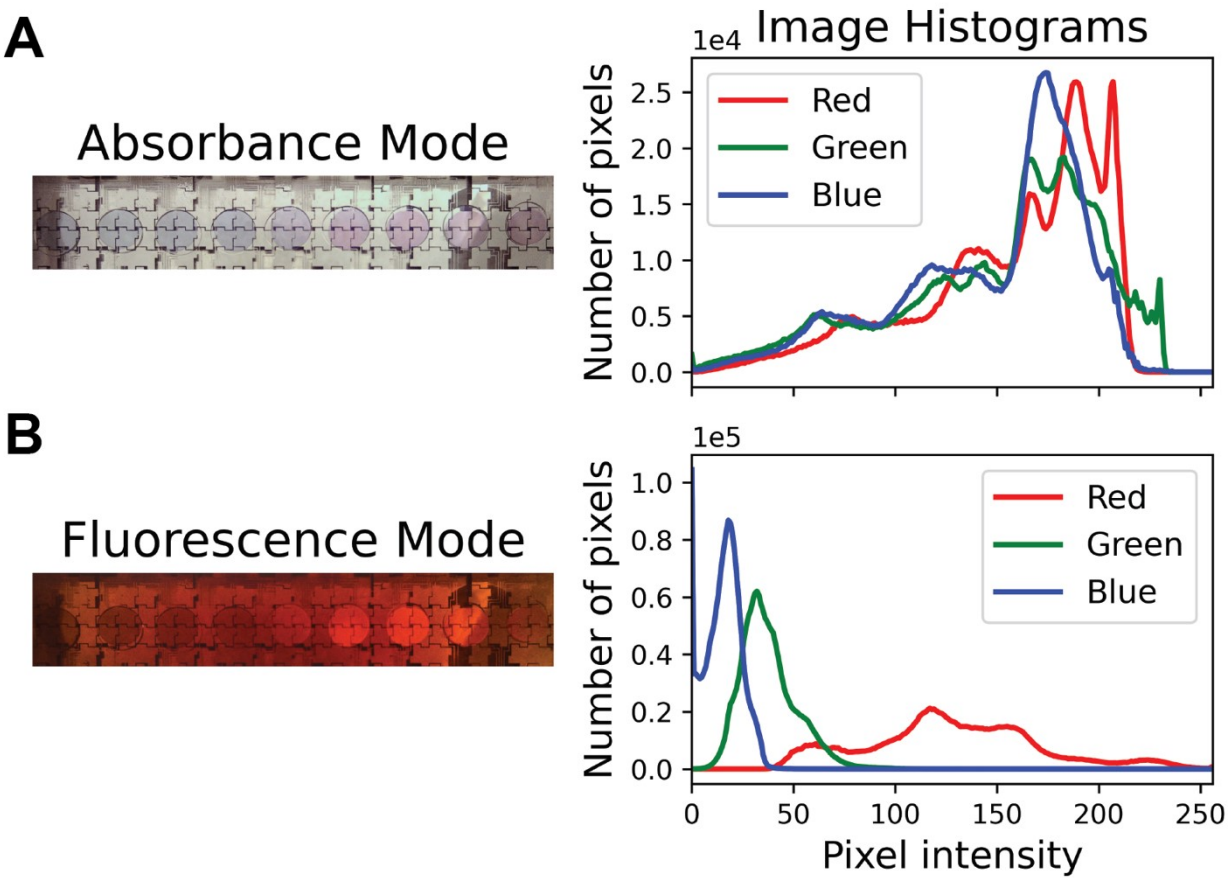

Fig. S7. Absorbance and fluorescence imaging modes. Left: Images captured from the same device bearing nine four-unit droplets during an AST experiment in which *E. coli* 1001728 was incubated with ciprofloxacin for approximately 4 h, under (A) Absorbance mode (white light illumination and no filter) and (B) Fluorescence mode (green illumination and filter). Right: The corresponding histograms for each of the images. Under fluorescence mode the green and blue channels are supressed by long-pass filter.

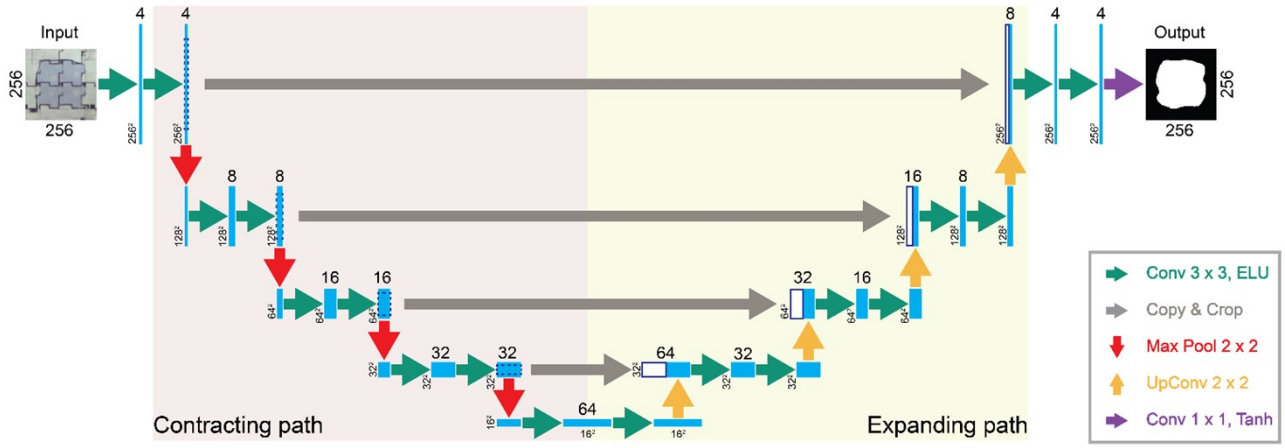

Fig. S8. Flowchart illustrating the custom convolutional neural network architecture used in this work. Each blue box corresponds to a multi-channel feature map. The input image was a square with dimensions of 256 × 256 pixels that consisted of three channels Red, Green, Blue. The x-y-size of each layer is indicated at the lower left edge of the box as a power of 2 since the x and y dimensions are equal. White boxes represent copied feature maps. The arrows denote the different operations: green arrows represent a convolution (padded convolution) using a 3 × 3 kernel followed by an Exponential Linear Unit (ELU), grey arrows represent copy and crop of feature maps from the layer to the left of the arrow to the layer to the right, red arrows represent max pooling using a 2 × 2 kernel for down-sampling, yellow arrows represent up-sampling using a 2 × 2 convolution ("up-convolution") and the purple arrow represents a final 1 × 1 convolution used to map each 4-component feature vector to the desired number of classes. The network had a total of 42 layers.

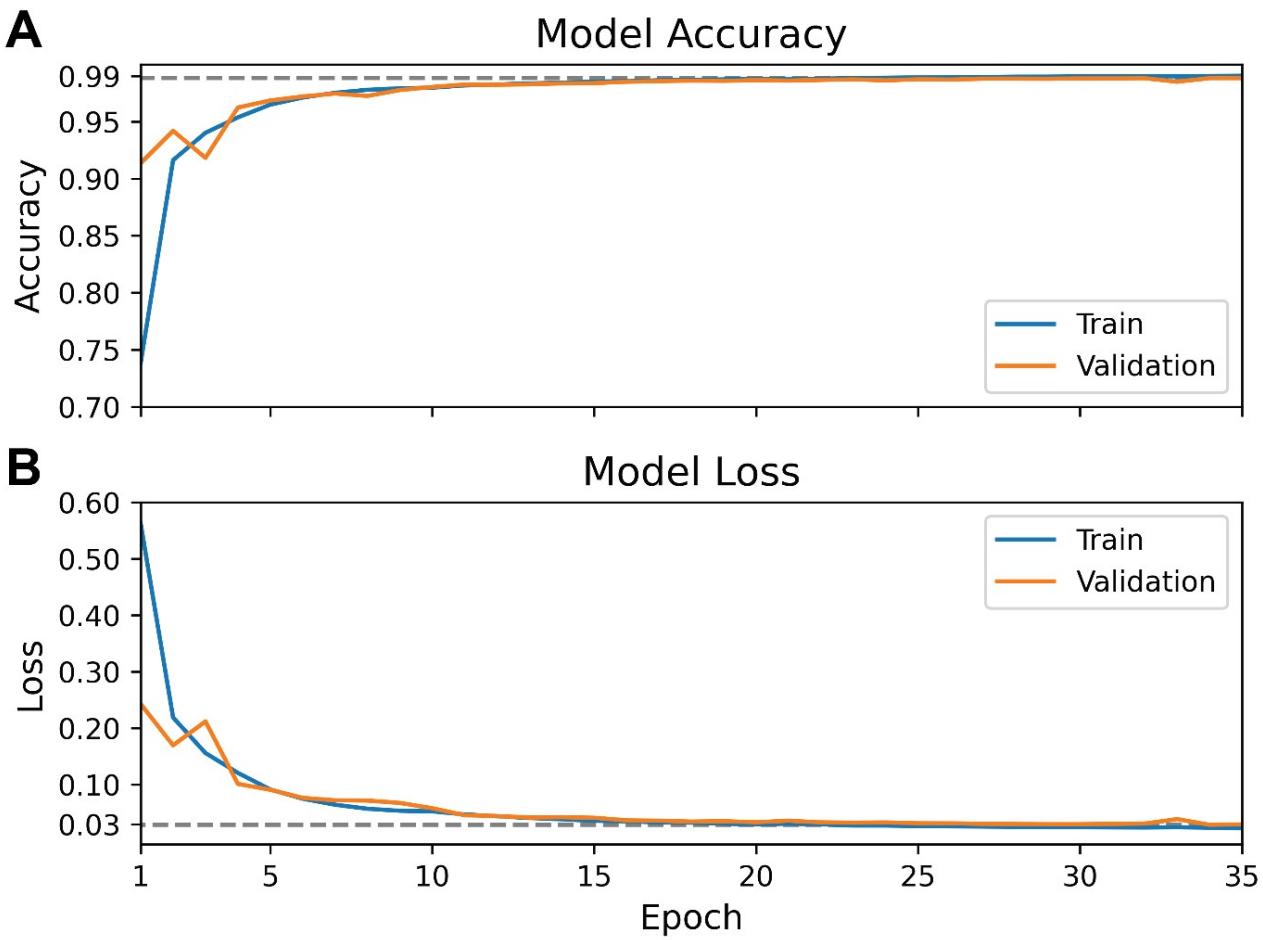

Fig. S9. Convolutional neural network performance over 35 training epochs. Blue lines indicate the performance of the training set and orange lines the performance of the validation set. (A) Graph of accuracy of the model; the dashed line indicates the maximum accuracy achieved for the validation set at 33 epochs. (B) Graph of model loss; the dashed line indicates the minimum loss achieved for the validation set.

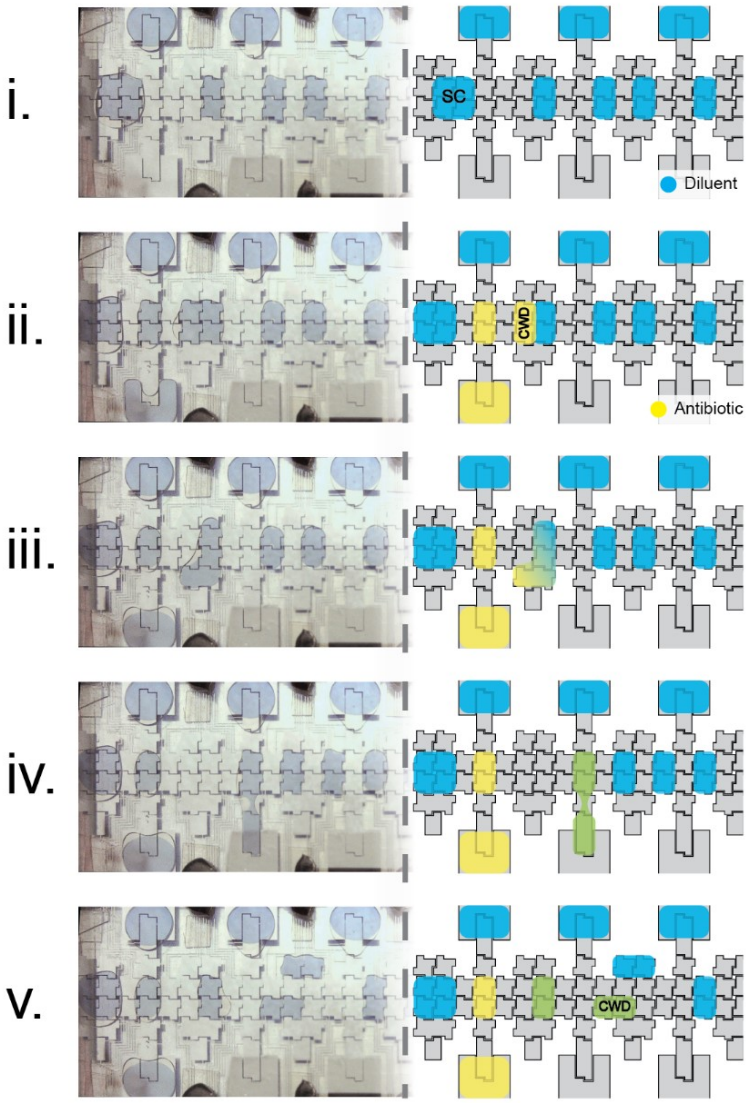

Fig. S10. Photos (left) and schematic representations (right) of the formation of a 2-fold antibiotic serial dilution series on DMF. (i) Two-unit droplets (2.2 µL) of diluent (MHB with 0.25 mM resazurin) are dispensed from reservoir electrodes and stored temporarily on the chip. A four-unit droplet (4.4 µL) is also dispensed to serve as a SC. (ii) Two two-unit droplets of a solution containing a known amount of an antibiotic in diluent are dispensed. One is stored temporarily on the chip (as the droplet with highest antibiotic concentration in the dilution series) and the other as the “concentrated working droplet" (CWD) (iii) The CWD is merged with an adjacent diluent droplet to form a four-unit droplet that is mixed for 1 min in a rectangular pattern involving 4 actuation electrodes and a mixing electrode. (iv) Upon mixing, the four-unit droplet is split into two equal two-unit droplets. (v) One two-unit droplet is stored temporarily on the chip (as a member of the dilution series) while the other two-unit droplet is the next CWD. Steps iii to v are repeated to generate the desired number of antibiotic dilutions on the DMF device; when step v is reached for the final dilution, one of the two two-unit droplets is stored on the device (as the droplet with lowest antibiotic concentration in the dilution series), while the other two-unit droplet is discarded.

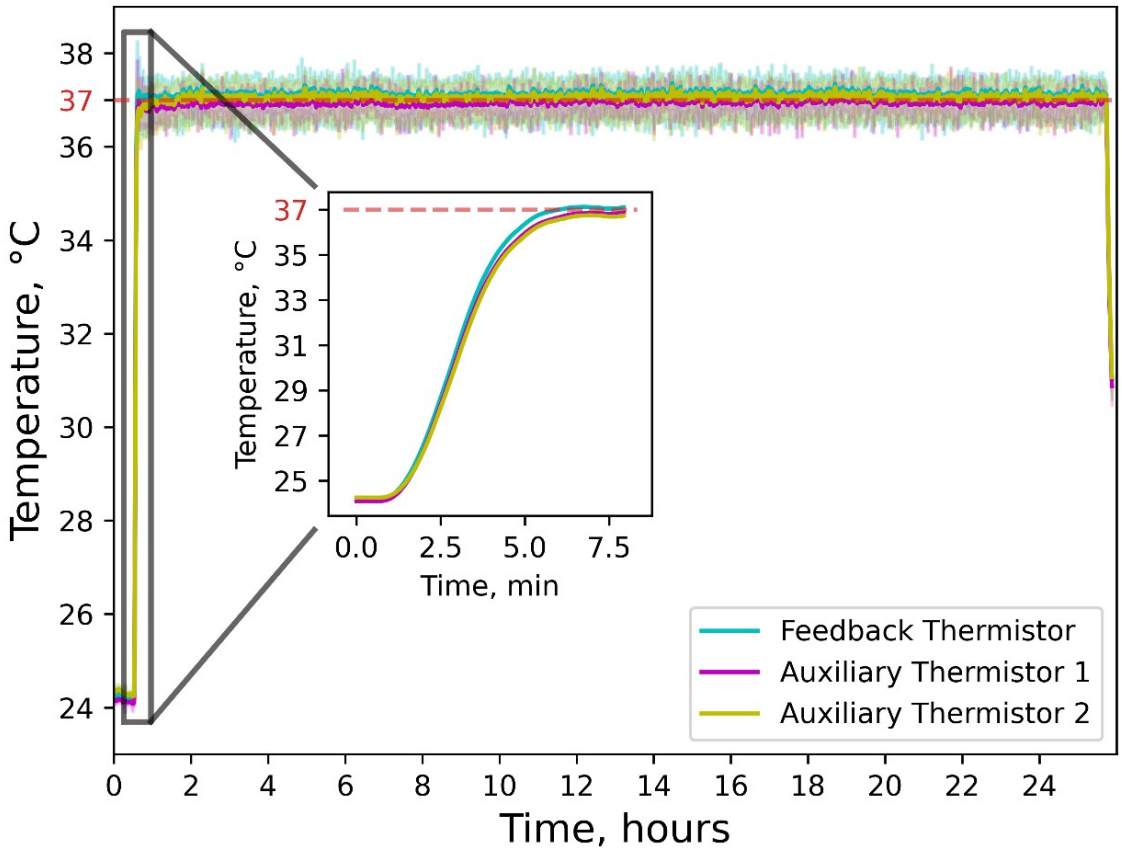

Fig. S11. Integrated temperature control. Plot of temperature measurements recorded over time by the three thermistors in the integrated system. The feedback thermistor (turquoise) is located in the middle of the heating block, closest to the middle of the DMF cartridge. The auxiliary thermistors (magenta, yellow) are aligned on either side of the feedback thermistor. In this experiment, temperature was set to 37 °C at 0 min and was held constant for 25 h. The inset is a magnified view of the data in the first 7.5 min after initiation.

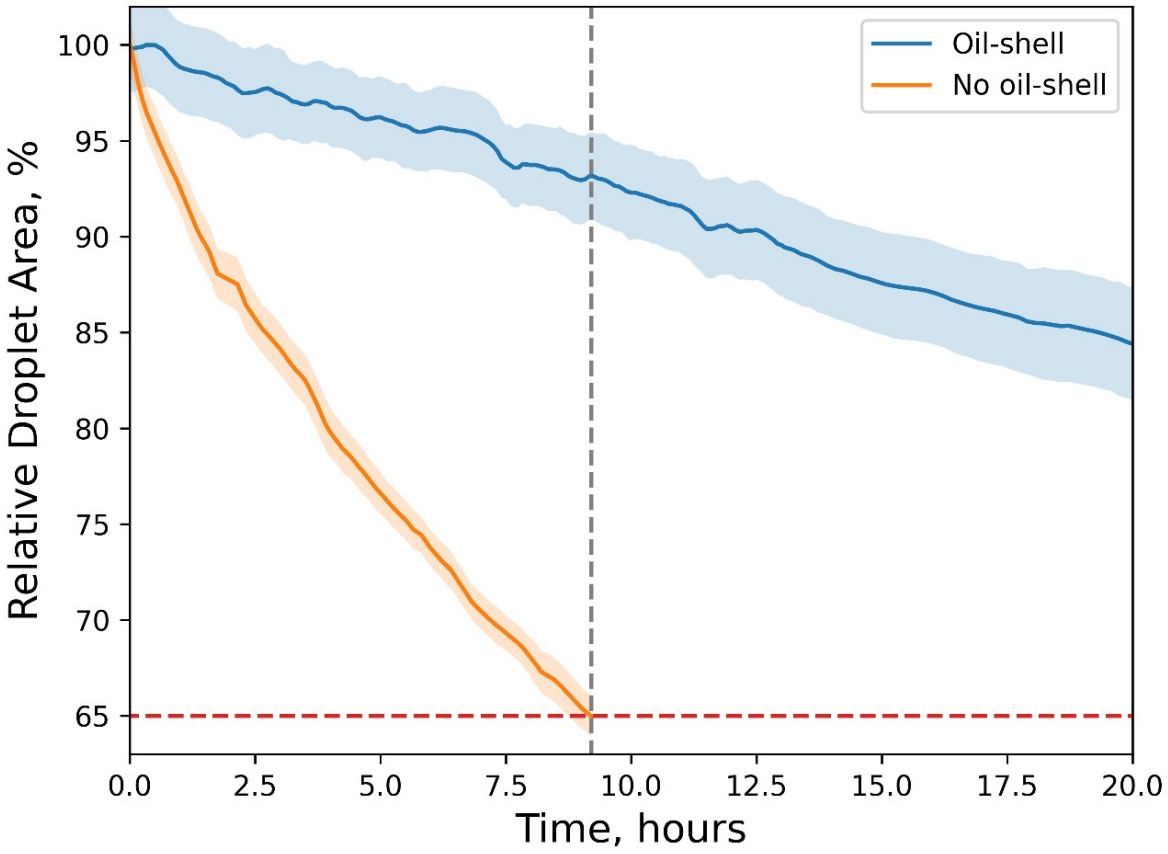

Fig. S12. Droplet stability on DMF. The CNN was used to identify droplet contours to generate a measure of relative droplet area with respect to time. Four-unit aqueous droplets of MHB with resazurin were evaluated in devices with humidified atmospheres, with (blue) and without (orange) encapsulation in immiscible shells of Vapor-Lock. Shaded regions represent standard error of n = 8 droplets. The red dashed line indicates the maximum evaporation threshold (35% relative droplet area loss) and the grey dashed line highlights the time point at which the relative droplet area reached the threshold in the absence of an oil shell.

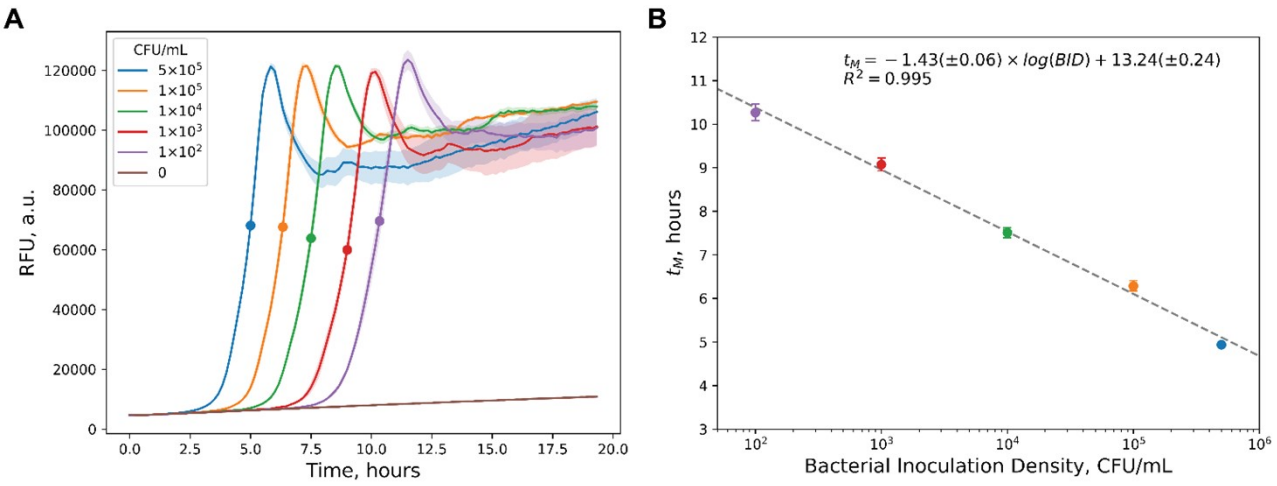

Fig. S13. Correlation between mid-point of sigmoidal resorufin curves with bacterial density. (A) Fluorescence intensities of resorufin as a function of time for samples inoculated with 5×10^5 (blue), 1×10^5 (orange), 1×10^4 (green), 1×10^3 (red), 1×10^2 (purple), or 0 (brown) CFU/mL *E. coli* CFT073. Shaded regions represent standard error of 3 replicates and the times required to reach the mid-point of each curve, t_M, is marked with solid circle. (B) t_M data from (A) plotted as a function of bacterial inoculation density (BID). Error bars represent standard deviation from replicate measurements of each condition (n = 3) and the grey line is a linear regression between the points. The fitted equation and the R^2 are included in the plot.

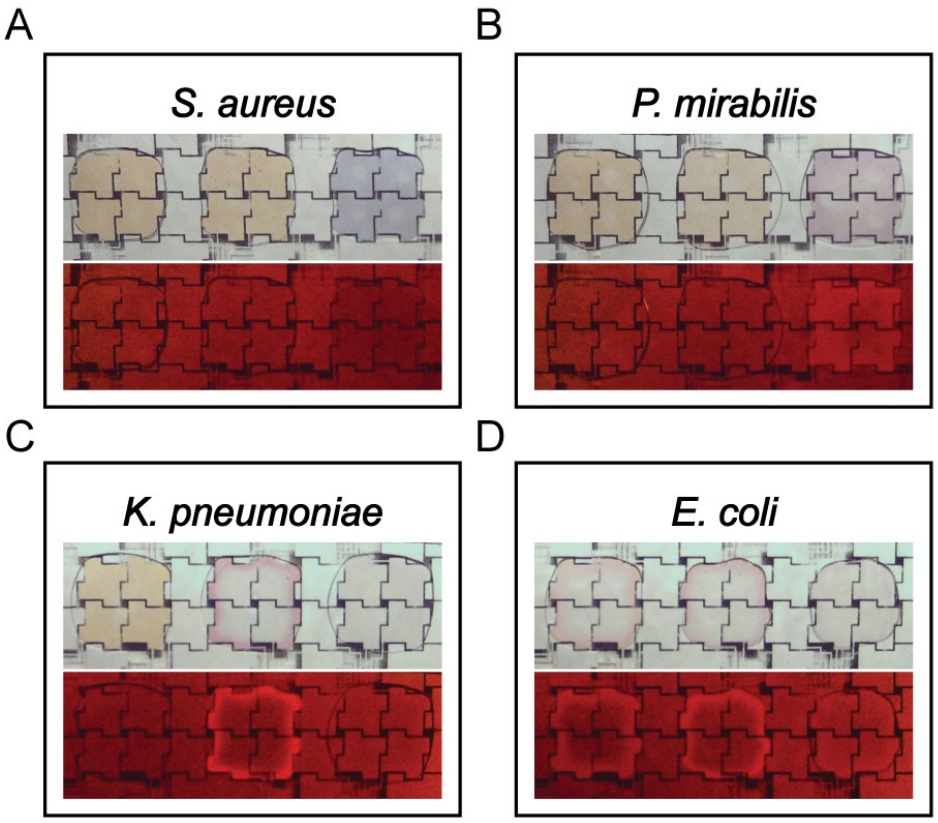

Fig. S14. DMF BC experiments. Representative images (Absorbance mode – top and Fluorescence mode – bottom) of three BC droplets of bacterial samples containing (A) *S. aureus* (at *t* = 6.0 h), (B) *P. mirabilis* (at *t* = 5.0 h), (C) *K. pneumoniae* (at *t* = 7.5 h), (D) *E. coli* (at *t* = 5.0 h). In each experiment, each set of three droplets contained REG (left-light orange), RGP (middle-orange), or resazurin (right-blue), which were converted to resorufin (pink and fluorescent) over time for classification of bacterial strains. Note the "halo effect" observed in some of the droplets containing *K. pneumoniae* and *E. coli* (in the fluorescent images).

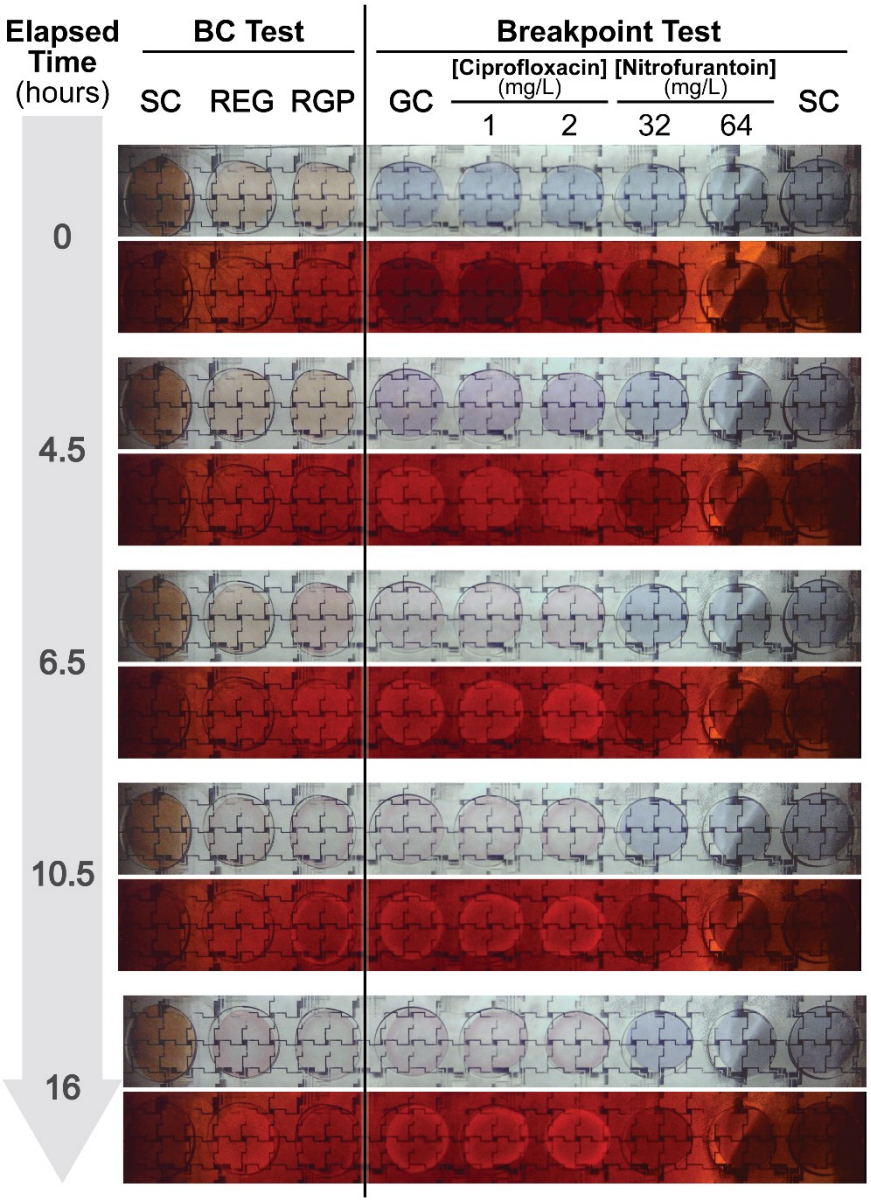

Fig. S15. Simultaneous breakpoint testing and BC on DMF. Representative absorbance (top) and fluorescence (bottom) images collected in an analysis of *E. coli* 1001728 at increasing time points (from top-to-bottom). The droplets contained (from left to right) REG and RGP only (sterility control for BC experiments), bacteria plus REG (for *E.coli* classification), bacteria plus RGP (for coliform classification), bacteria plus resazurin (bacterial control for breakpoint testing), bacteria plus resazurin and ciprofloxacin (1 mg/L and 2 mg/L), bacteria plus resazurin and nitrofurantoin (32 mg/L and 64 mg/L), and resazurin only (sterility control for breakpoint testing). The antibiotic concentrations were selected to corelate with known susceptible (S) and intermediate (I) breakpoint concentrations, to classify bacteria as susceptible (no growth in either droplet), intermediate (growth at the lowest antibiotic concentration only), or resistant (growth at both antibiotic concentrations).

Table S1. Nitrofurantoin AST determination via standard broth microdilution reference method.

Strain	Nitrofurantoin MIC (mg/L)
E. coli 1001728	8 Susceptible[a]
E. coli CFT073	8 Susceptible

[a] In category agreement with ATCC® datasheet (susceptible). ['ATCC® NDM-1 Strains', 2014]

Table S2. Ciprofloxacin AST determination via standard broth microdilution reference method.

Strain	Ciprofloxacin MIC (mg/L)
E. coli 1001728	128 Resistant[a]
E. coli CFT073	0.015[b] Susceptible
K. pneumoniae ATCC® 700603™	0.5[c] Susceptible
S. aureus ATCC® 29213™	0.25[d] Susceptible
P. mirabilis ATCC® 29906™	0.12[e] Susceptible

[a] In category agreement with ATCC® datasheet (resistant). ['ATCC® NDM-1 Strains', 2014] [b] In essential agreement with reported literature value (0.03 mg/L). [Chockalingam et al., *Antibiotics*., 2019, **8**, 170] [c] In essential agreement with reported literature value (0.5 mg/L). [Rasheed et al., *Antimicrobial Agents and Chemotherapy*., 2000, **44**, 2382–2388] [d] Within the reported range of MICs by the CLSI (0.12-0.5 mg/L). [Clinical and Laboratory Standards Institute, 2015] [e] In essential agreement with reported literature value (0.125 mg/L). [Aiassa et al., *FEMS Microbiology Letters*., 2012, **327**, 25–32]